



Recharge estimation from discrete water-table datasets in a coastal shallow aquifer in a humid subtropical climate

Fabrizio Rama¹ · Konrad Miotlinski¹ · Davide Franco¹ · Henry X. Corseuil¹

Received: 10 October 2017 / Accepted: 30 January 2018
© Springer-Verlag GmbH Germany, part of Springer Nature 2018

Abstract

A time-series approach to the estimation of recharge rate in unconfined aquifers of highly variable water level is proposed. The approach, which is based on the water-table fluctuation method (WTF), utilizes discrete water-level measurements. Other similar techniques require continuous measurements, which makes them impossible to apply in cases where no data from automatic loggers are available. The procedure is deployed at the Ressacada Farm site, southern Brazil, on a coastal shallow aquifer located in a humid subtropical climate where diurnal water-level variations of up to 1 m can follow a precipitation event. The effect of tidal fluctuations on the groundwater levels is analyzed using a harmonic component builder, while a time-variable drainage term is evaluated through an independent analysis and included in the assessment. The estimated recharge values are compared with those obtained from the continuous measurements showing a good agreement with the approaches for discrete dataset intervals of up to 15 days. Subsequently, the estimated recharge rates are incorporated into a transient groundwater-flow model and the water levels are compared showing a good match. Henceforth, the approach extends the applicability of WTF to noncontinuous water-level datasets in groundwater recharge studies.

Keywords Water-table fluctuation method · Groundwater recharge/water budget · Numerical modeling · Tidal influence · Brazil

Introduction

Accurate estimation of groundwater recharge is of relevance for different applications related to the assessment of human activity and hydrogeological characterization. It may be critical information to manage changes in groundwater systems effectively (Xiao et al. 2016) and to safeguard scarce resources in arid zones (de Vries and Simmers 2002). Proper estimation of recharge and its variability in time and space is shown to be crucial for both the agricultural sector (Bohlke 2002) and the assessment of fate and transport of solute pollutants (Kim et al. 2000), since it can induce temporal fluctuations in the flow field. Spatial and temporal variability in recharge, as well as

preferential flow paths, are key components for assessing aquifer vulnerability to a specific compound (Scanlon et al. 2002). Many investigators deal with the relationship between recharge estimation and numerical groundwater models (Colombani et al. 2016; Sanford 2002), focusing on the main role of vadose flow for simulating recharge (Cao et al. 2016; Heilweil et al. 2015). For a humid climate, Hunt et al. (2008) showed similar timing of recharge but an appreciably different water budget when considering thin unsaturated zones in the simulation. The literature reports a multitude of methods being developed and commonly used to infer recharge (Healy 2010). Recharge is part of the overall infiltration mechanism, when the wetting front reaches the water table, causing its rise. Precipitation is the main forcing of the process, and it is an important factor in the recharge estimation (Shi et al. 2015). Theoretically, in a uniform porous medium with a shallow water table, it can be assumed that a fraction of total precipitation in a time step contributes to the aquifer recharge (Park and Parker 2008), resulting in a prompt rise of water level in shallow unconfined aquifers (Hilberts et al. 2007). The deeper the water table, the greater the amount of rainfall water held in the unsaturated zone, which in consequence leads to a reduction of the precipitation fraction reaching the water table and

Electronic supplementary material The online version of this article (<https://doi.org/10.1007/s10040-018-1742-1>) contains supplementary material, which is available to authorized users.

✉ Fabrizio Rama
fabrizio.rama@posgrad.ufsc.br

¹ Department of Environmental Engineering, Federal University of Santa Catarina (UFSC), Florianopolis, SC 88040-900, Brazil

to a time lag between the forcing and water-table rise. Realistically, estimation of groundwater recharge is an iterative process, involving multiple approaches with progressive aquifer-response data collection and resource evaluation (de Vries and Simmers 2002). For this reason, despite this abundance of solutions, assessing the accuracy of any applied method (Healy and Cook 2002) and choosing the most appropriate for given field conditions (Scanlon et al. 2002) is still extremely difficult.

The water-table fluctuation method (WTF) is a widely used method (Masetti et al. 2016; Saghravani et al. 2015) which requires the knowledge of groundwater levels to estimate recharge. Usually applied in an event-basis framework (Delin et al. 2007; Lorenz and Delin 2007), WTF is a simple method applied for unconfined aquifers with a shallow water table and sharp variation in water level. There are three principal requirements for the use of WTF (Healy 2010; Healy and Cook 2002): (1) the applied time step must be as short as possible, (2) an accurate value of specific yield must be used (Acharya et al. 2012; Nachabe 2002), and (3) other possible causes of groundwater head fluctuations not related to recharge must be isolated from the dataset (Neto et al. 2015). In order to estimate recharge useful for aquifer water-balance calculations, a time series approach for WTF has been developed by Crosbie et al. (2005) showing a reliable and well-founded methodology. Nevertheless, its application for continuous datasets presents two major limitations: (1) the empirical estimation for groundwater drainage by a linear function of depth may not properly explain the spatial and temporal variability of the flow field (Cuthbert 2010), and (2) the model requires a continuous and homogeneous level dataset with sufficiently high temporal resolution, at least with hourly records.

Although hydrogeologists constantly deal with a lack of data, there is a tendency to neglect historical databases with incomplete and disjointed information. Nevertheless, discrete records of water-table depth can bring some useful information if they are treated using correct methodologies. This paper extends the application of the time series approach (Crosbie et al. 2005) for discrete hydraulic head datasets. To address this issue, a variable drainage term (D term) may be introduced as an exponential function of the time elapsed from the last rain event, explaining water head reliance of discharge in the time domain. To verify the whole procedure, recharge estimates from a couple of piezometers are compared with those obtained from continuously monitored water-table series and integrated in a transient 2D vertical flow model. In addition, a harmonic component analysis of high-frequency residual signals is included in the analysis to assess the astronomical tide influence on the groundwater levels in the area, excluding other processes responsible for water-table rises. This contribution aims to clarify the uncertainties in recharge estimates with WTF from discrete records and explains how to

extract useful groundwater information from irregular datasets.

Site description

An unconfined aquifer at the Ressacada Farm experimental site, in the southwestern part of Santa Catarina Island, southern Brazil, is studied (Fig. 1a,b). The aquifer, 30–40 m thick, is fairly homogeneous consisting of lacustrine deposits with a predominance of fine quartz sand with lenses of silt and clay (De Lage 2005). The total area is 20 km² and the aquifer is laterally adjacent to (1) an Atlantic channel called South Bay to the north and west (Garbossa et al. 2014), (2) the slow curvy estuarine system of the Tavares River surrounded by mangrove swamps to the east, and (3) a compact granite complex of hills to the south (Fig. 1c). The groundwater flow is a result of a very low natural gradient driven by precipitation recharge, and is radial diverging from the domain center to the boundaries.

The ground surface is flat (up to 5 m in elevation) and the average depth to water level varies from 0.3 to 2.0 m. The aquifer constitutes a u-shaped groundwater system (Huang et al. 2015; Mao et al. 2006) which is enclosed on three sides by natural surface water bodies subjected to boundary tidal fluctuations, carried by tidal channels and swamp dynamics. A dense network of artificial trenches in the plain drains the top of the shallow aquifer maintaining the water level below the topographic surface.

From a meteorological point of view, the region is located in the humid subtropical climate zone under the Köppen-Geiger classification (Peel et al. 2006) at the contact of the Atlantic moist tropical and Antarctic polar air masses. The interactions and alternations between the fronts cause rainfall events with high intensity and large variability (Grimm et al. 1998). Precipitation is predominantly in the summer season, and the monitored annual rainfalls varied from 1,100 to 2,700 mm between years 2007 and 2017. The large variability of rainfall results in large and quick fluctuations of the groundwater levels.

The majority of water-level measurements come from the Experimental Area 3 (Fig. 1d), which was historically used to conduct biofuel remediation experiments (Corseuil et al. 2015, 2011a). Average hydraulic conductivity values are in the range of 10⁻³ cm/s. Mean total porosity, measured by gas permoporosimetry, is 0.38 ± 0.01 (*n* = 31). The effective porosity (η_e) of the saturated soil is 0.2 (Corseuil et al. 2011b), while the moisture content of the unsaturated zone profile varies from 20 to 25% (De Lage 2005). In this part of the aquifer the flow field occurs along section A–A' to the SE, toward the Tavares River (Kobiyama et al. 2011), and is affected by recurring variations in recharge intensity due to the following—the shallow depth of the water table; the porous

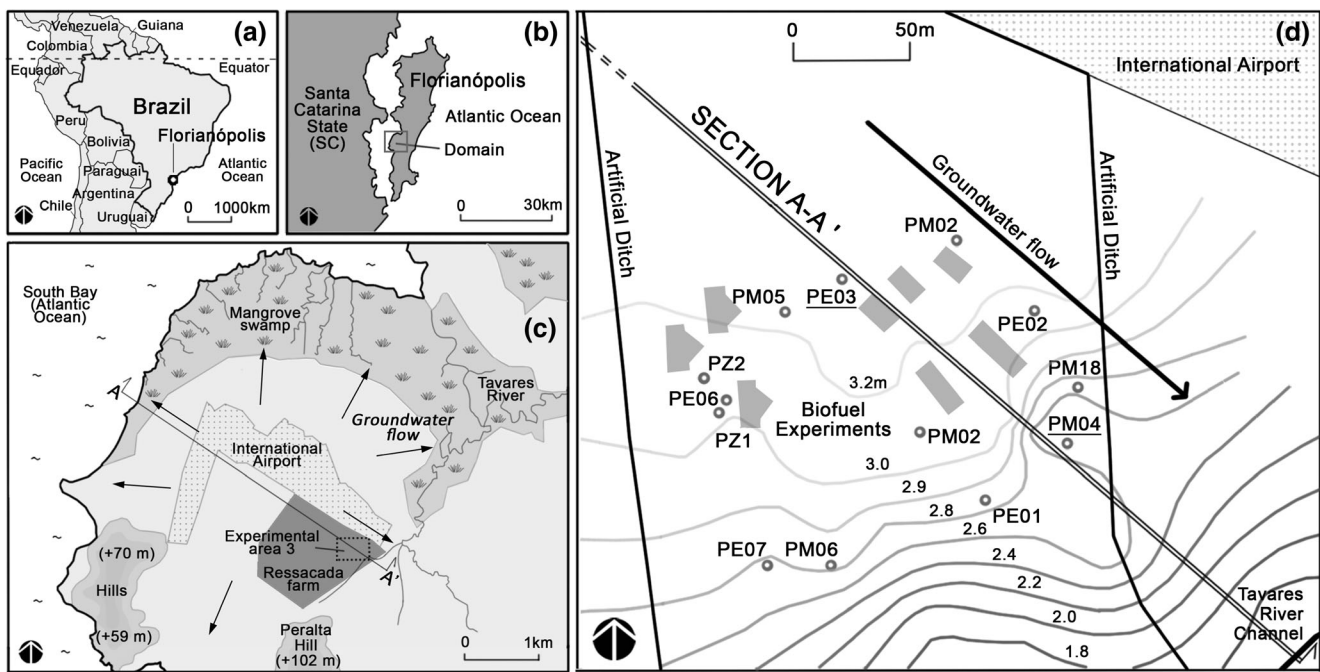


Fig. 1 Location of study area: **a** map of Brazil; **b** map of Santa Catarina Island; **c** study domain at Ressacada Farm Experimental Site, with boundary conditions. Section A–A' indicates the domain transect; **d** Detailed map of Experimental Area No. 3, depicting: piezometer

positions and their names (points), topography with elevation in meters above mean sea level (lines and numbers), and natural attenuation experimental areas (gray areas)

highly conductive nature of the deposits; the intermittent, intense and spatially variable nature of rainfall; and the proximity to boundary receptors. Experimental Area 3 is approximately 3 km from South Bay, 2 km from Ribeirão Bay, and less than 500 m from the Tavares River; nevertheless, the area is located far away from intensive anthropogenic activities, with no pumping, and steep hydraulic gradients. For these reasons, the aquifer satisfies the conditions to apply the WTF for recharge estimations (Healy and Cook 2002) which are: (1) lack of confinement with sharp temporal water-level changes; (2) large number of piezometers to observe water levels; (3) no pumping and no anthropogenic activities that may influence the natural groundwater level over short time scales; (4) a short time lag, and intense and variable rainfall events.

Materials and methods

Methodology

A discrete dataset of water levels from 13 piezometers measured from 2007 to 2016 is used in the study (Table 1). Most of the wells in the area are shallow piezometers that intercept the aquifer up to a depth of 4.5 m, with the exception of PZ01, PZ02 and PE06, which reach 15, 10 and 30 m in depth, respectively. Water-table depths were monitored with a manual phreatimeter at variable recording intervals (1–60 days). In

addition, in a shorter time window (from 8 February 2017 to 31 March 2017), PE03 and PM04 are equipped with automatic water-level loggers, recording every 15 min. Both wells are supplied with a vented pressure transducer of a range of 3.5 m with an accuracy of $\pm 0.1\%$; therefore, the instruments automatically correct the measurements by pressure, to be vented, and by temperature deviation, with a linearizing algorithm of two known points; hence, the resulting total error is in the order of ± 2 mm.

The WTF is based on the premise that water-table rises are due solely to vertical rainfall infiltration (Healy and Cook 2002); therefore, in a time step Δt , a total amount of recharge R [mm] is mathematically defined as:

$$R = S_y \times \frac{\Delta h}{\Delta t} \quad (1)$$

where S_y is the specific yield [% by volume], and Δh is the maximum registered water-level change [mm] in a time step Δt . A recharge ratio RR [%] is:

$$RR = \frac{R}{P} \quad (2)$$

where P is the total amount of rainfall [mm] in the same time step Δt . The P represents total precipitation including events not contributing to water-level rises, whereas R refers to the sum of all level rises in the same period. In accordance with Eq. (1), all the components in the groundwater budget that are not storage (like evapotranspiration, net subsurface flow or

Table 1 Piezometers and their design details

Name (Ref. code)	Ground elevation ^a , MSL ^b [m]	Well screen depth (top/bottom) [m]	Well screen elevation ^c , MSL (top/bottom) [m]	Well case diameter [cm]
PE01	2.83	2.5/4.5	0.3/−1.7	5.08
PE02	3.20	2.5/4.5	0.7/−1.3	5.08
PE03 ^d	3.30	2.5/4.5	0.8/−1.2	5.08
PE06	3.10	20.0/30.0	−16.9/−26.9	10.16
PE07	2.72	11.0/13.0	−8.3/−10.3	11.43
PM01	3.32	2.5/4.5	0.8/−1.2	5.08
PM02	3.24	2.5/4.5	0.7/−1.3	5.08
PM04 ^d	2.50	2.5/4.5	0.0/−2.0	5.08
PM05	3.32	2.5/4.5	0.8/−1.2	5.08
PM06	2.88	2.0/4.0	0.9/−1.1	5.08
PM18	2.66	1.0/3.0	1.7/−0.3	5.08
PZ01	3.12	10.0/15.0	−6.9/−11.9	5.08
PZ02	3.19	5.0/10.0	−1.8/−6.8	5.08

^a *Ground elevation*: values obtained with a Geodetic total station (distance accuracy of 5 mm and angular de 2")

^b *MSL*: elevation above Mean Sea Level (zero reference at the ground control point of Imbituba Sea Level Station)

^c *Well screen elevation*: equal to *Ground elevation* minus *Well screen depth*

^d Piezometer used as an observation point in 2D model

baseflow) are supposed null during the recharge process. The time lag between the arrival of the infiltrated water and its redistribution to all the components is place-specific and determines the reasonable time step to be applied in the method. Therefore, over cumulative time intervals (months or years), all the contributions that are not accounted in the recharge term, like evapotranspiration losses and surface runoff during the precipitation, are lumped in (1-RR), with RR defined in Eq. (2). Using the WTF, recharge values are inferred in variable time steps along a time window of 10 years. A variable drainage rate and variations of S_y with depth are included in the evaluation. The time series approach by Crosbie et al. (2005) is modified to handle discrete datasets with irregularly spaced data. This is to handle heterogeneity of datasets which made it difficult to directly compare one-by-one data using statistical methods available in the time-series analysis (Neto et al. 2015).

The paper follows three main stages. In the first part, the recharge values are estimated on the basis of water-level fluctuations using a sparse, discontinuous and time-variable dataset with time intervals varying from 1 to 60 days. In the second part, the estimates are compared with the continuous time-series approach (Crosbie et al. 2005). Finally, in order to verify the assumptions, test the conceptual model and calculate water balances, a numerical model was built with a finite element method (FEM), the FEFLOW code (Diersch 2014).

Discrete-series approach

Discrete and irregularly spaced records of water-table levels are used to automate the estimation of monthly accumulated

recharge. In accordance with the work of Shi et al. (2015), which indicates precipitation as the most important factor controlling the daily and monthly WTF recharge estimates, the following conditions are applied in the approach:

$$R_{\Delta t_i} = (\Delta h_i + D\Delta t_i) \times S_{ya} \xrightarrow{\text{if}} \sum_{\Delta t_i} P_d > 0 \text{ and } (\Delta h_i + D\Delta t_i) > 0 \quad (3)$$

where Δh_i represents the ‘differenced water level’ in each interval [mm], that is the difference in water head between two consecutives records, D is the drainage rate [mm/d] or D term, Δt_i is the interval time length [d], P_d is the daily accumulated precipitation [mm], and S_{ya} is the apparent specific yield [% by volume], estimated by Eq. (5). Subscript i represents all intervals available in the dataset; hence, the recharge value in Eq. (3) is estimated in the rainy intervals solely, and is corrected by all drainage contributions lumped in the D term, including the moisture content of the unsaturated zone. The term substitutes, at each interval, the drawing of the “antecedent recession curve” that the well hydrograph would have followed in the absence of the rise-producing precipitation (Healy and Cook 2002; Fig. 2a), in analogy with the Master Recession Curve approach (Delin et al. 2007).

The methodology is divided into five basic steps. Firstly, the series are synchronized and the measurements are consolidated to remove errors or outliers. In order to avoid underestimation of recharge (Delin et al. 2007) sampling intervals longer than 15 days are excluded, losing only 1% of records; therefore, the resultant average sampling interval used in the procedure is 3–4 days. Secondly, the raw depth dataset is

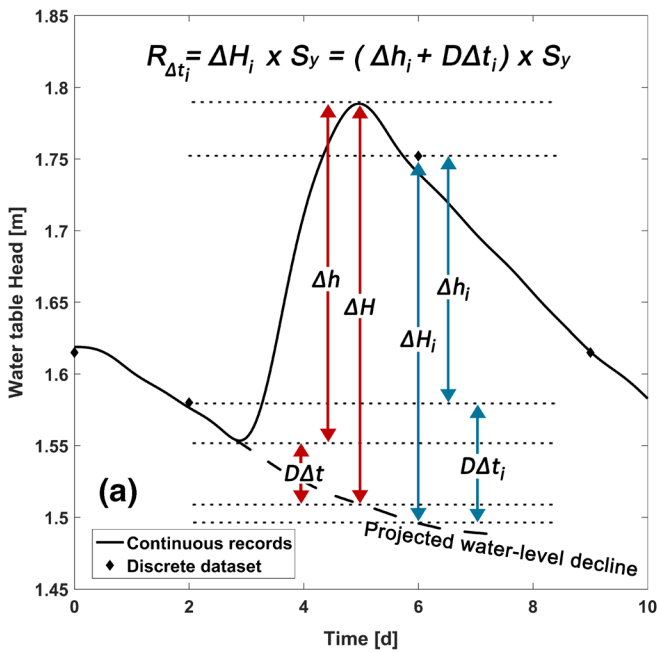
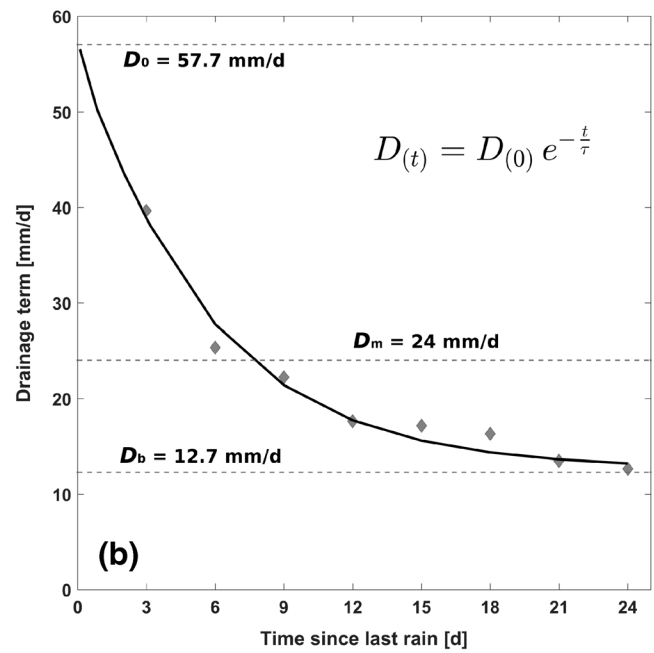


Fig. 2 Conceptual model sketches: **a** Definition of the WTF for continuous (red arrows) and discrete (blue arrows) datasets: ΔH_i represents the total water-table rise in the interval, whereas Δh_i is defined according to the water-level measurements; **b** Exponential model (equation) fitted on field data to assess the D term as a function of the time elapsed since the last rainfall. Solid line is the mean function



obtained from the fitting curves of 13 piezometers, gray diamonds represent for each time step the mean drainage value for the whole dataset, D_0 is the average initial drainage after a rainfall event, D_m is the median drainage and D_b is the average low-head drainage for long periods without rain (adapted from Rama et al. 2017)

converted to absolute hydraulic head above mean sea level. Thirdly, the difference in water levels between consecutive measurements (Δh_i) is defined. Then, the amount of rainfall in each interval [mm] is calculated as the sum of the daily precipitation (P_d) between the first day and the second to last day of the interval as in Eq. (4).

$$P_{\Delta t_i} = \sum_{\Delta t_i} P_d \xrightarrow{\text{if}} \sum_{d=1}^{N-1} P_d \text{ with } (\Delta t_i = t_1, t_2, \dots, t_N) \quad (4)$$

Finally, accumulated precipitation is used to divide the time-series: intervals with null accumulated precipitation are isolated and used to determine the rates related to the drainage processes where no recharge occurred, while intervals with positive accumulated precipitation are used to infer the recharge itself.

As derived analytically by Cuthbert (2010) groundwater drainage in a flat unconfined aquifer is a transient function depending on the distance from (a) the surface receptor and (b) water-table head. The water head dependency of drainage (D term) in the Ressacada Farm site is explained as an empirical exponential function with respect to time for a period of 10 years (from 2007 to 2016; Rama et al. 2017). Since a linear relationship between saturated volume and groundwater discharge at quasi-steady-state conditions was suggested (Walker et al. 2015), it was proposed to group the rates into classes representing time elapsed since the last rain event. In order to simplify the procedure these averaged values are used in the

discrete approach of WTF to infer recharge. Thus, upper and lower drainage values in a significant time-scale obtained from the average best-fit curve for the whole area are as follows: 12.7 mm/d for the low-head drainage of the aquifer in dry periods, and 57.7 mm/d immediately after a rainfall event, when the hydraulic head of the aquifer is high (Fig. 2b). As shown in Fig. 2b, low-head drainage indicates the water-table decreasing rate after 24 days with no rain, since dry periods never overstepped 25 days in 10 years of monitoring. In the continuous approach of WTF, a constant D term is set up to 24 mm/d, equal to the median of the whole distribution of drainage rates.

An apparent specific yield (S_{ya}) represents the storage of water controlled by capillary forces above the water table, assuming a transient nonideal release of water (Childs 1960; Duke 1972). Mathematically, for a layered soil S_{ya} is defined as (Crosbie et al. 2005):

$$S_{yu} = (\phi - S_r) \rightarrow S_{ya} = S_{yu} \frac{S_{yu}}{[1 + (\alpha \times d)^n]^{1-\frac{1}{n}}} \quad (5)$$

where ϕ is the total porosity, S_r is the specific retention, also known as field capacity [% by volume], d is the mean depth of the water table in the time step [cm], and S_{yu} is the ultimate specific yield [% by volume]. To determine S_{ya} a nonlinear relation between soil moisture and specific yield is assumed, supposing pressure distribution at equilibrium at each step. Given the spacing of the sampling intervals and a quick

reaction of the water table to the rainfall, this strategy seems reasonable. S_{yu} represents a steady specific yield without influence of depth. Soil specific parameters of the Van Genuchten moisture model (α and n) are adopted from the Hanford sediment (Eching and Hopmans 1993) which exhibits similar characteristics and behavior with the Ressacada soil. In order to estimate S_{yu} , the procedure by Armstrong and Narayan (1998) is automated for a discrete dataset, obtaining ultimate specific yield from the groundwater level changes versus the accumulated precipitation plot (Fig. 5). To assess S_{yu} , only the water level declines in the last 50 cm of recorded depths in each piezometer are used. This corresponded to the water-table depth of at least 1.5 m; therefore, only the low-head drainage value of 12.7 mm/d is applied to lower records. Finally, multiplying the differenced water level series corrected with the drainage term by the S_{ya} , the recharge in each interval is inferred and aggregated in a monthly recharge at the Ressacada farm.

Continuous analysis and tidal frequency analysis

In the second stage, the discrete-series approach is compared with the continuous-series analysis proposed by Crosbie et al. (2005). The analysis is performed for the datasets PE03 and PM04 in a 51-day time window, from 8 February 2017 to 31 March 2017 (Fig. 3), using both manually collected records (discrete and variably spaced data) as well as datalogger series (continuous and homogeneously spaced data). The two piezometers are chosen to be located along the main groundwater flow direction and exhibit the highest difference in the water-table variability.

To manage continuous datasets, water level records are firstly resampled to 1-h rate using a Doodson filter (Pugh 1987). This is followed by a data synchronization for the period from 8 February 2017 at 15:00:00 to 31 March 2017 at 09:00:00, to obtain 1,220 hourly records. In a congruence analysis, errors, spikes and noise are removed. To isolate periodic components with high frequencies, a Low Pass 33 filter (LP33) is subsequently applied (Emery and Thomson 2001). Finally, in order to separate tidal influence from other periodic contributions (evapotranspiration, atmospheric pressure variation, etc), a frequency analysis is carried out with a MATLAB-based UTide code (Codiga 2011) on the residual signal (red lines in Fig. 3). The harmonic component builder allowed one to identify the signal contribution at tidal frequencies from time series, including groundwater records. In addition, UTide is run on the sea level series, monitored in the South Bay, comparing the identified significant components with the PE03 and PM04 results. The significance of each component is attributed to the amplitude of the signal, based on the accuracy of the sensors and the signal-to-noise ratio (SNR) with a modified Rayleigh criterion, while their relative importance is controlled by the percent energy (PE) contributing to the signal reconstruction (Codiga 2011). The SNR value of 6 and a minimum PE of 0.5% are adopted. The sea levels in the South Bay are monitored by an OTT/RLS radar level sensor (accuracy of 3.5 mm, sampling frequency of 5 min) and are provided by EPAGRI/CIRAM (Agricultural Research and Extension Company/Information Center for Environmental Resources and Hydrometeorology).

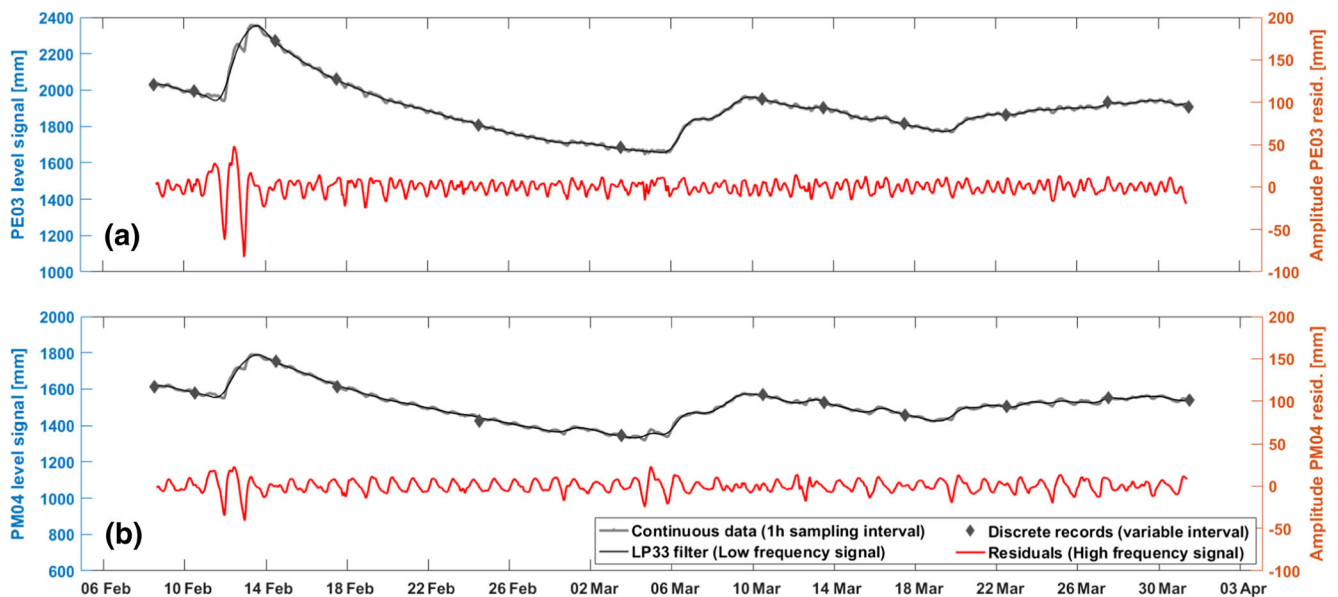


Fig. 3 Comparative plot of raw data (gray lines and diamonds), the Low Pass 33 filter signal (black line), and high frequencies residuals (red line) for **a** PE03 and **b** PM04 in the 51-day period. The residual signal is analyzed with UTide (Codiga 2011) to assess astronomical tide influence on the water table

Numerical FEM model

In the last stage, a 2D vertical finite element model is constructed in order to integrate obtained recharge estimates in a transient simulation of the flow field. The model domain of 3,650 and 32 m in length and height, respectively, is divided into 18,154 rectangular elements (58 rows and 313 columns), regularly spaced in the horizontal direction every 11.7 m and with irregular spacing in the vertical direction. In the top 5.2 m of depth, the spacing is equal of 0.4 m and then increased gradually by about 5.5% until the bottom. The elevation $z = 0$ m refers to the mean average sea level. At the elevation $z = 2.4$ m the domain is divided into two layers of different hydraulic properties to reflect the existence of a superficial layer of finer geologic material rich in organic matter.

Constant-head boundary conditions (Dirichlet-type BC) are used to represent surface water bodies: South Bay on the left side ($x = 0$ m; $z = 0$ m), and Tavares River on the right ($x = 3,650$ m; $z = 0.8$ m). In addition, five “seepage face” BCs are introduced within the domain to represent partially penetrating artificial ditches at an elevation $z = 2.8$ m ($x = 944$, 1,236 and 2,460 m), at $z = 2$ m ($x = 3,180$ m), and at $z = 1.2$ m ($x = 3,500$ m; Fig. 4). Conceptually, a seepage face corresponds to a constant-head BC, which is combined with a

maximum flux constraint equal to zero, allowing a free out-flow of water from the model. To reproduce a parallel trench influencing the flow field, but located outside of the simulation domain, a Cauchy flow BC constrained with a null max-flow rate is used (Diersch 2014). This condition allowed for the performance of a distance-dependent drain in the central part of the domain from $x = 1,294$ m to $x = 2,402$ m at an elevation $z = 3.4$ m. Finally, recharge is represented by a fluid-flux BC on the top elements, which is a time-variable inflow condition. These values express volumes of water traveling through the unsaturated zone to the water table, solved by Richard’s Law and regulated by a modified van Genuchten moisture model. The details of the model set up are presented in Table 2.

The model is calibrated using a trial-and-error method with the following criteria: (1) modeled hydraulic conductivity values should not deviate from the field-derived values by more than $\pm 15\%$; (2) hydraulic conductivity values are adjusted for the steady-state comparing simulated levels with the average of monitored hydraulic heads; (3) the initial condition of hydraulic head for transient-state is obtained by a single calibrated steady-state run; (4) unsaturated-flow porosity of layer 1 for the transient-state should not deviate by more than $\pm 15\%$ from the average of S_{va} estimates; (5) unsaturated-flow porosity of layer 2 and Richard’s model parameters are

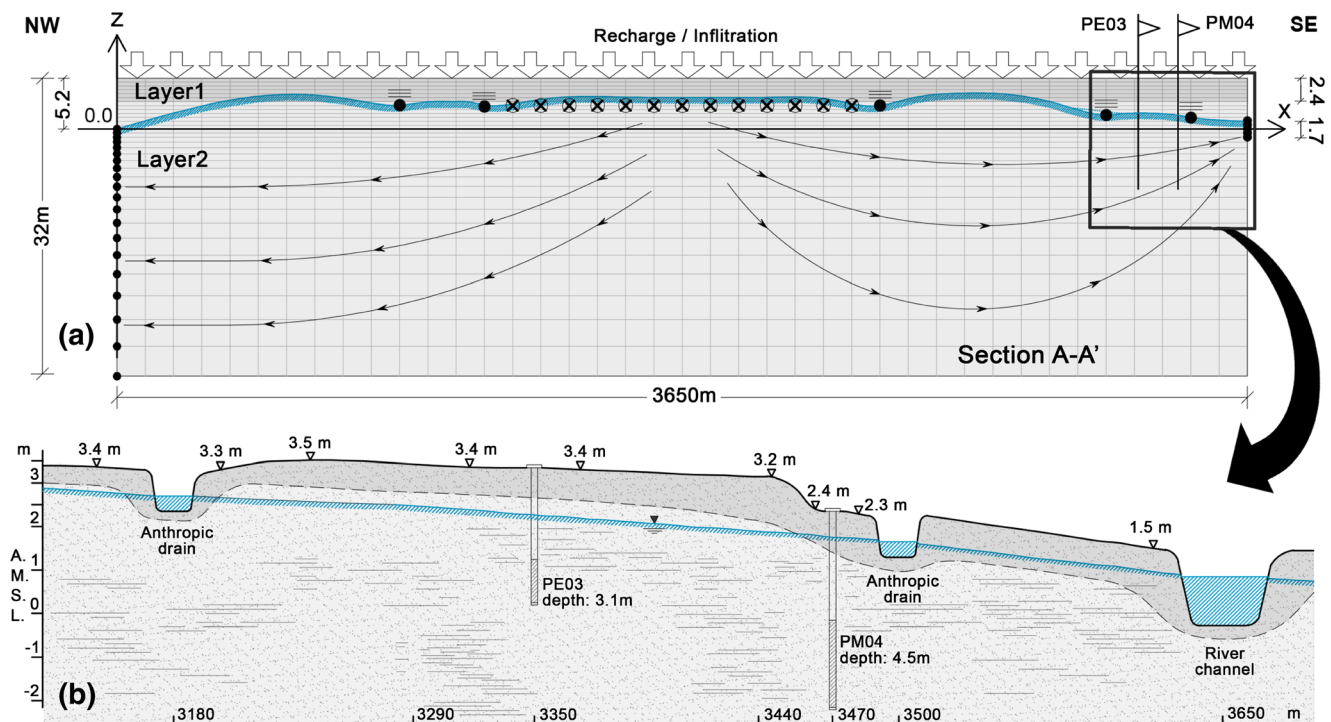


Fig. 4 **a** Two-dimensional (2D) finite element model setup along section A–A’ (Fig. 1c), used to test the recharge estimation methodology in stage 3. Filled dots represent the head boundary condition (BC), dots with lines above are constrained-head BC (seepage face), encircled crosses indicate Cauchy-type BC with flow constraint, lines with arrows show

groundwater flow paths, blue line is the water-table position, and flags are observation points (piezometer locations). **b** The detailed vertical section of the Experimental Area 3 (Fig. 1d), showing ground elevation and water-table position

Table 2 The two-dimensional FEM model input parameters and conditions

FEM parameter	Symbol	Value [unit]	Reference
Model parameters for “calibrated scenario”			
Saturated conductivity	K	3.2 (layer 1)/8.5 (layer 2) [m/d]	De Lage (2005)/field data
Unsaturated flow porosity	ϵ	0.067 (layer 1)/0.13 (layer 2) [-]	WTF estimation/calibration
Specific storage coeff.	S_0	0	Diersch (2014)
Maximum saturation	ss	1	
Residual saturation	sr	0.25	WTF method/field data
Modified van Genuchten parametric model			
Pore-size distribution index	n	2.2 [-]	Diersch (2014)
Fitting coefficient	α	2.8 [1/m]	
Fitting exponent	m	0.55 [-]	
Fitting exponent	δ	1 [-]	
FEM - 2D mesh consisting of 18,154 quadrangle elements (313 × 58)			
Domain	X vs Z	3650 vs 32 [m]	Conceptual model
Vertical space increment	Δz	0.4 + (5.5% Δz_{i-1}) [m]	
Horizontal space increment	Δx	11.661 [m]	
Initial time-step size	Δt_0	0.001 [d]	
RMS error tolerance (AB/TR)	ξ	0.001 [-]	
Simulation time period	t_{end}	52 [d]	

FEM finite element method model, design by the FEFLOW code (DHI); RMS root mean square

adjusted using a fixed RR into the range established with the WTF estimates in PM04 and PE03, equal to 43% of monitored precipitation (Table 3; Fig. 7); (6) daily recharge values in transient-state must not exceed precipitation; (7) approximation of hydraulic heads never oversteps minimal targets of 0.85 for the Nash-Sutcliffe (NS) efficiency coefficient, 10% of total observed head range for root-mean-square error (RMSE), and 10 cm of absolute error in comparison to field data (Anderson et al. 2015).

Therefore, once the model results satisfactorily represent transient hydraulic head data, scenarios with different recharge are constructed:

1. Recharge equal to 43% of daily precipitation, statistically inferred from rainfall records, and input parameters in compliance with Table 2 (also known as “calibrated scenario”)
2. Recharge assessed with the continuous-series method of WTF (section ‘Discrete-series approach’)
3. Steady constant recharge equal to 2.15 mm/d (43% of average precipitation in the 51-day period)
4. Recharge equal to 43%, with a constant unsaturated-flow porosity for the whole domain, equal to 0.188 (measure of S_{yu} estimated as the inverse of the slope of the line of best fit in Fig. 5)

Table 3 Comparison between discrete and continuous dataset estimations within the 51-day period

Dataset	Accumulated column [mm]	Recharge ratio [%]
Precipitation	260	–
PE03 discrete WTF	146	56.2
PE03 continuous WTF	136	52.3
PM04 discrete WTF	90	34.6
PM04 continuous WTF	81	31.2

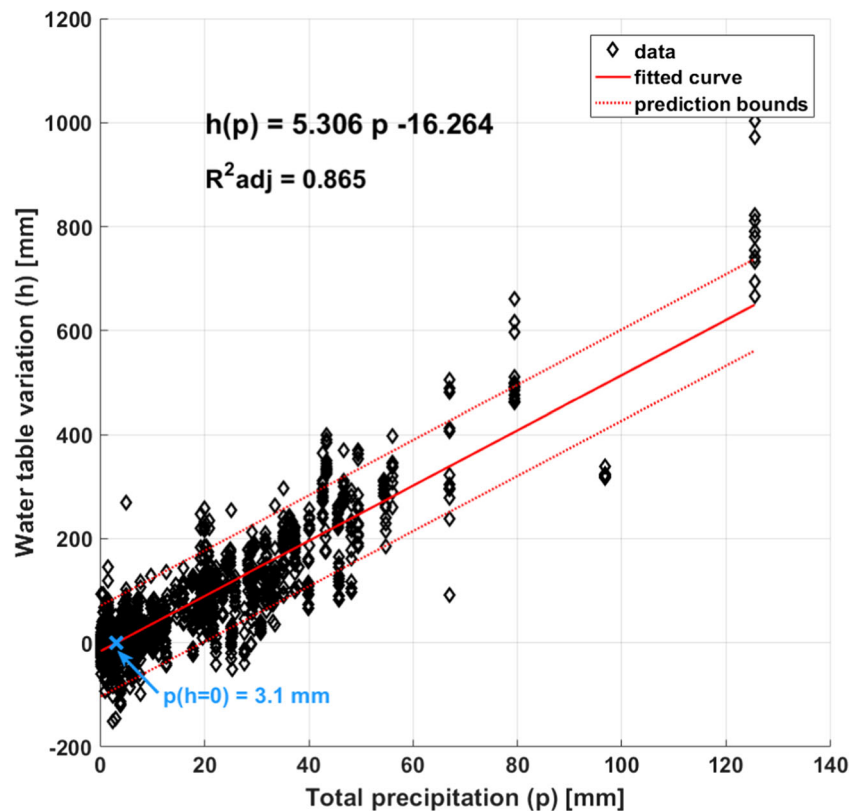
Results and discussion

Recharge estimation by the discrete and continuous approach to WTF

The water-level variations versus accumulated rainfall for each interval show a linear correlation (Fig. 5). The inverse of the slope of the fitting line in the graph gives the value of S_{yu} equal to 0.188 (95% confidence bounds from 0.185 to 0.192), which agrees with the field S_y assessment (Corseuil et al. 2011b).

All water losses (i.e. soil moisture variation, evapotranspiration and run-off) are assumed to be included in the part of the rainfall that falls below the threshold value (x-intercepting value in blue Fig. 5). This means that on average only accumulated precipitation above 3.1 mm (2.5–3.7 mm with 95% confidence interval) has an evident influence on the Ressacada groundwater levels.

Fig. 5 Ultimate specific yield estimation using the regression best fit (red line and equation) in a precipitation vs water-table fluctuation plot. R^2_{adj} is the degree-of-freedom adjusted coefficient of determination for the typed equation. Dotted lines show the prediction interval for a non-simultaneous new observation with 95% level of certainty



The estimates of average monthly recharge for the whole area show an outstanding variability (Fig. 6). There is no constant or directly proportional relation between monthly precipitation and recharge which has a three-fold explanation: firstly, in rainy months the intense runoff, due to the temporal proximity of precipitation events to each other, has less contribution to a water-table rise; secondly, recurrent flooding events during the intense precipitation periods reduces groundwater recharge; finally, swamp areas near the Tavares River modify hydraulic head to boundary receptors for long periods resulting in a reduced capacity for aquifer drainage, and hence, storage capacity. It should be highlighted that, since months with no available water level records are excluded from the analysis, no bar of recharge is shown in the graph for these months. For the discrete dataset of 13 piezometers the total recharge in 10 years varies from 5,634 to 6,957 mm which constitutes from 38.5 to 47.2% of precipitation, respectively; this is on average 43% of RR in the area (Fig. 7).

The values of monthly recharge sums indicate that average annual recharge varies between 536 to 885 mm/year, respectively, for the driest and wettest year, whereas the annual recharge range (difference between maximum and minimum value) between all the piezometers is on average 230 mm. Therefore, average recharge ratios are in the range of 35.9–51.6%, resulting in a wider range of RR than the 10-year analysis; additionally, it should be emphasized that the years

with more accumulated rainfall show the lower RR values. This suggests that the effectiveness of recharge decreases with the increase of precipitation, due to an enhanced saturation of pores; an effect widely referred to as “fill and spill” systems (Tromp-van Meerveld and McDonnel 2006). The implication is that dry winter months show on average markedly higher RR, whereas during the rainy months RR is lower.

Recharge estimates for the continuous datasets during a 51-day time span are 136 and 81 mm for PE03 and PE04, respectively. The recharge estimates in the same period for the discrete datasets are 146 and 90 mm for PE03 and PE04, respectively, showing a good agreement between the approaches (Table 3).

The sensitivity analysis of inferred recharge ratios (RRs) to the model parameters is summarized in Table 4. In the column headings, RRs in parentheses refer to the whole 10-year time period for the different S_{yu} values and D term. The recharge estimates with WTF exhibit a linear relationship with S_{yu} value, as shown in Eq. (5). Nevertheless, if S_{yu} is constant (no S_{ya} decline at the surface) recharge estimates increase dramatically, which is an observation that confirms the finding by Child (1960), indicating an overestimation of recharge if a constant S_y is used instead of a non-steady value. In addition, the model seems to be very sensitive to the drainage term, highlighting the importance of its accurate assessment. The D term has increasing influence depending on the larger time step between the records. Similarly, uncertainties on the real recession

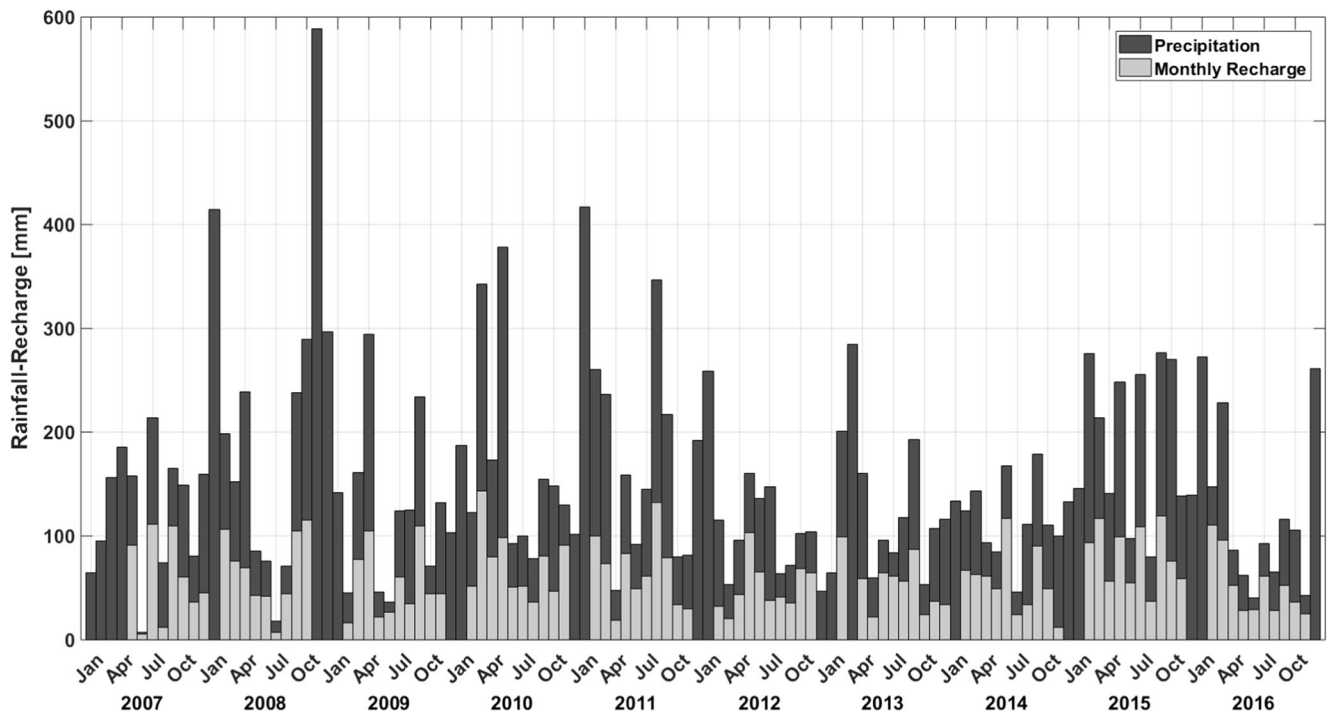


Fig. 6 Comparative bar plot between monthly recharge estimates (light bars) and total precipitation (dark bars). Recharge bars are average values between the 13 piezometers

hydrograph intensify their relevance in the final estimation; thus, for this reason, the authors suggest to use head-variable D values up to 1 week, adopting a fixed low-head or median D value for time intervals overstepping 1 week.

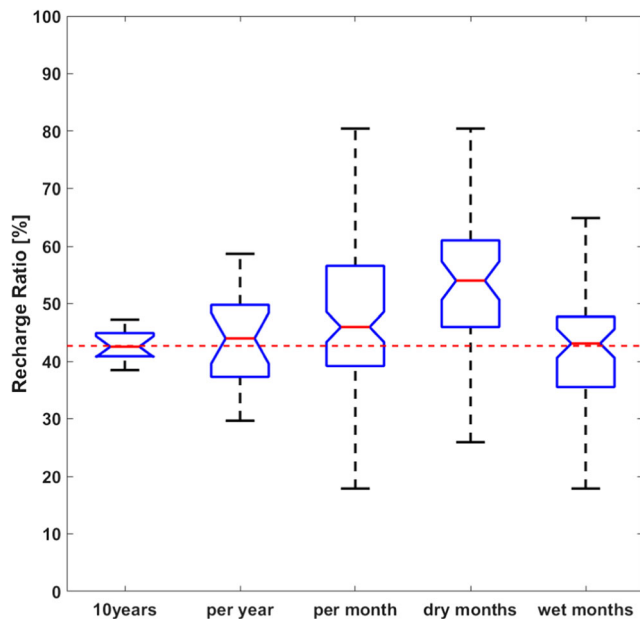


Fig. 7 Statistics boxplot of estimated recharge ratio (RR) for different time periods. Red lines express median value of distribution; blue boxes indicate the 25th and 75th percentiles, while dashed whiskers extend to the most extreme data points. Red dashed line show 43% (median RR in 10 years)

Integration of WTF results into the FEM model

Observed and simulated water head values in PM04 and PE03 show a good agreement (Fig. 8), with a NS coefficient of 0.87 and a RMSE of 5 cm. Solid lines in the graph represent calibrated simulation with parameters as in Table 2 and RR equal to 43% of daily precipitation (scenario 1). Recorded precipitation and water-table variation (dashed lines) indicate a generally fast response of the Ressacada aquifer to infiltration forcing (8–24 h). The distribution of simulated levels (solid lines) indicates a similar timing in recharge in agreement with findings by Hunt et al. (2008). In addition, the comparison of

Table 4 Summary of sensitivity analysis results

S_{yu} (RR) ^a [% by volume]	D term (RR) ^a [mm/d]
0.188 (0.430)	Initial values: 12.7–57.7 ^c (0.430)
0.13 (0.302)	Constant low-head value: 12.7 (0.357)
0.2 (0.464)	No correction with D term: (0.248)
0.2 constant ^b (0.794)	Constant average value: 20.7 (0.441)
	Higher piezometer: 15.2–66.2 ^c (0.483)
	Lower piezometer: 9.6–35.9 ^c (0.390)

^a RR in brackets is the average recharge ratio between all piezometers, calculated as the ratio of total recharge in 10 years and total accumulated precipitation

^b Constant specific yield equal to field assessment (Corseuil et al. 2011b)

^c Respectively, final and initial drainage rate in an exponential D function of 25 days without rain, namely 24-dry-days and 0-dry-days drainage

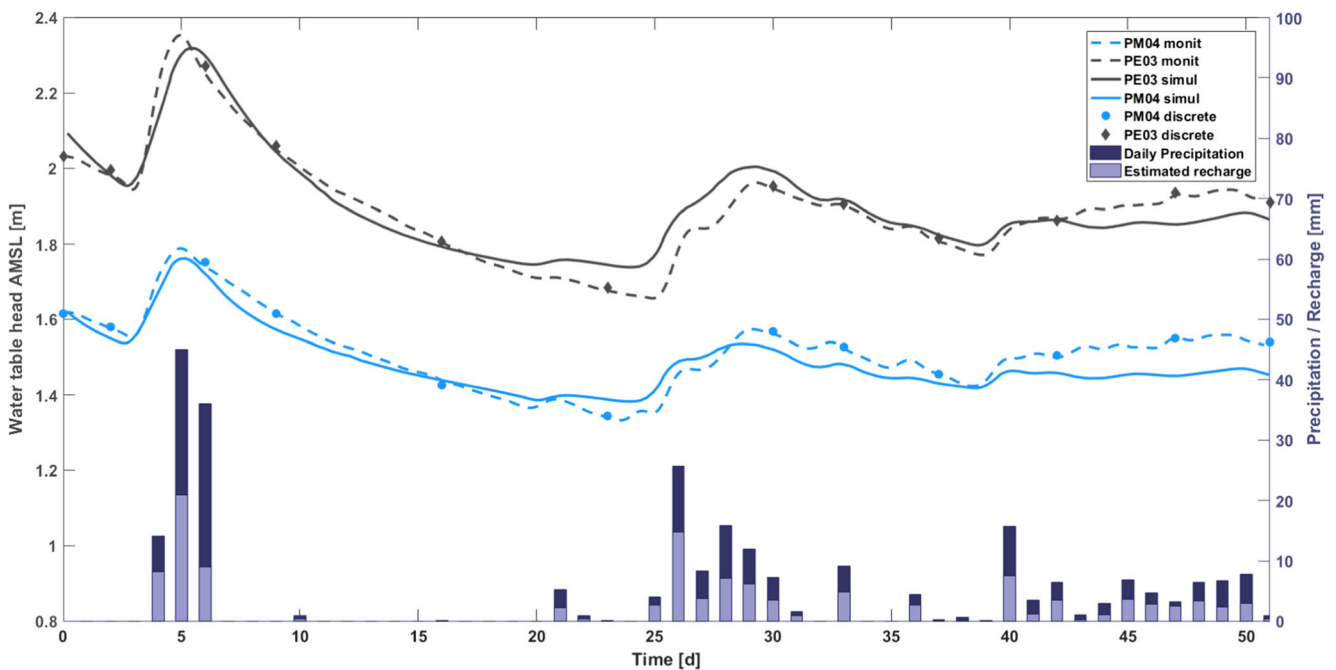


Fig. 8 Combined plot showing water level fluctuations in the 51-day period. Dashed lines represent continuously monitored piezometer levels, while solid lines are the calibrated asset (scenario 1). The bar

plot shows recorded precipitation (dark purple bars) and daily estimated recharge values (lilac bars)

records from two piezometers exhibits greater distance between the two lines during a rainfall event and immediately after it, with a scarce increase of PM04 levels compared with levels at PE03. This behavior demonstrates the spatially different recharge in the area, with greater fluctuations in areas further away from the boundary receptors.

The numerical model allows one to compare water budget components between the estimated recharge with WTF and different FEM scenarios. Comparative analysis of the water columns at the end of the simulation (Fig. 9) shows a good agreement in the water budgets with the WTF estimates (Table 3). Although the NS coefficient on the water-table head decreases from 0.87 to 0.76 passing from scenario 1 to scenario 2—see the electronic supplementary material (ESM)—water volumes at the end of the simulation are very close in both runs. It suggests that prior estimation of recharge with WTF prevents a long trial-and-error process to assess the recharge with the numerical model, also providing a robust theoretical basis for its values. The difference in the shapes of the “rainfall recharge” curves (Fig. 9) emphasizes that effectiveness of recharge is related to the precipitation distribution: first, a more intensive rainfall event (days 4–6) has less estimated RR than 43% and the curve grows less, whereas the second event (days 25–31), less rainy and more distributed in time, exhibits a higher RR than the average value of 43%.

The calibrated scenario 1 was also tested using a transient unsaturated flow porosity in layer 1 equal to the estimated S_{ya} , as described in section ‘Discrete-series approach’ (see ESM).

Here, the water budget exhibits sharper curves in response to changing parameters along the simulation, with a higher contribution of storage volume to flow between days 9 and 25. Nonetheless, the total approximation of simulated levels results in a NS coefficient of about 0.77. It should be highlighted that the storage contribution to flow at the end of 51 days remains similar in all the scenarios, except with a constant unsaturated-flow porosity equal to S_{yu} (scenario 4). By running this scenario (see ESM), hydraulic levels, and hence, water discharge budgets show a pronounced sensitivity to the parameter, with a drastic mismatch in the peak of hydrographs (absolute error more than 15 cm), although the simulation NS efficiency coefficient remains about 0.8. This explains the sensitivity of recharge estimates using WTF to the value of S_{yu} (Table 4). Finally, by running the “steady recharge” run (scenario 3), simulated steady-state levels converge to the average of the transient hydraulic head in scenario 1, with also good agreement in the entire water budget at the end of the simulation (see ESM).

Using scenario 1, model verification is run on a 10-year-long discrete dataset of groundwater levels for PE03 and PM04 (Fig. 10). The resulting water table shows a good model agreement for the majority of water level values, except for low water levels for which modeled values are overestimated. The head-BC assigned on Tavares River is meant to represent a natural dynamic system with sharp level fluctuations over time. In accordance with the head-dependent relationship of Darcy’s Law, the BCs define in the model the hydraulic gradient for nodes where flow occurs, mostly in long periods

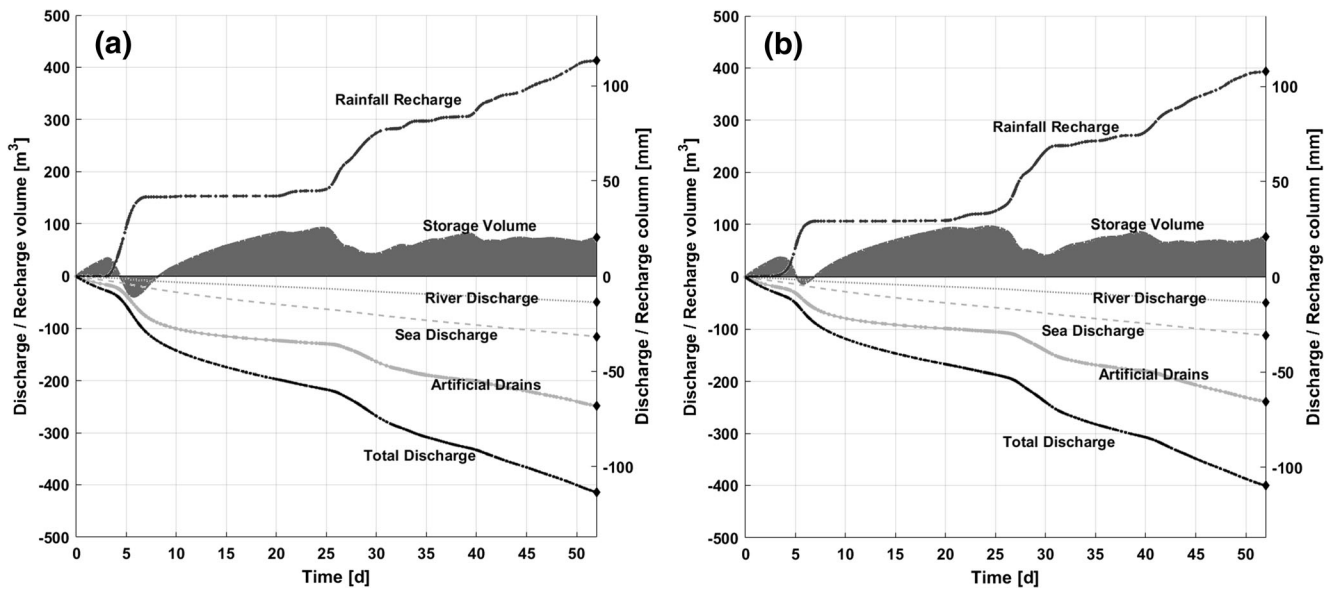


Fig. 9 Transient cumulative groundwater balance: **a** scenario 1, **b** scenario 2. Storage filled curves exhibit storage contribution to flow and discharge

without rainfall. This behavior implicates a progressively slower flow as the water table approaches an equilibrium state with the BCs; however, dry periods determine lower levels in the river too, resulting in a faster decrease of groundwater levels in the field, which are impossible to simulate with fixed values of BCs. Therefore, the authors suppose that the deviation could be reduced with the use of a time-variable boundary condition at the river cells rather than a time-constant value;

nevertheless, the deviation from the field data occurs in periods of null recharge only, and, hence, it is of a low significance for long-term recharge estimation.

Tidal influence assessment

Frequency decomposition of the groundwater-level signals indicates an only marginal tidal influence on PE03

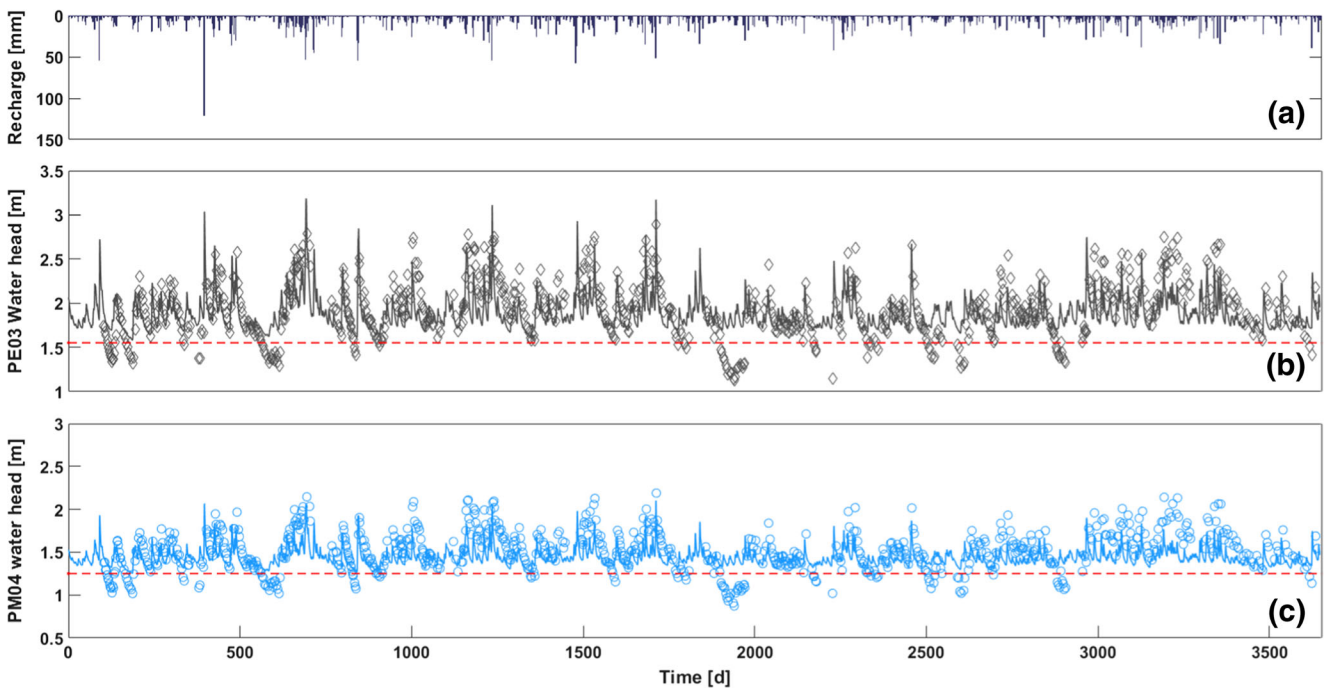


Fig. 10 2D model verification plot: comparison between simulated (solid lines) and monitored levels dataset (symbols) in a 10-year-long simulation that used calibration parameters, for **a** recharge, **b** PE03, **c** PM04. The red dashed lines (lower head value reached by simulation in

each piezometer) show that simulated lines never decrease under fixed values related to the river BC, losing accuracy to explain low groundwater levels

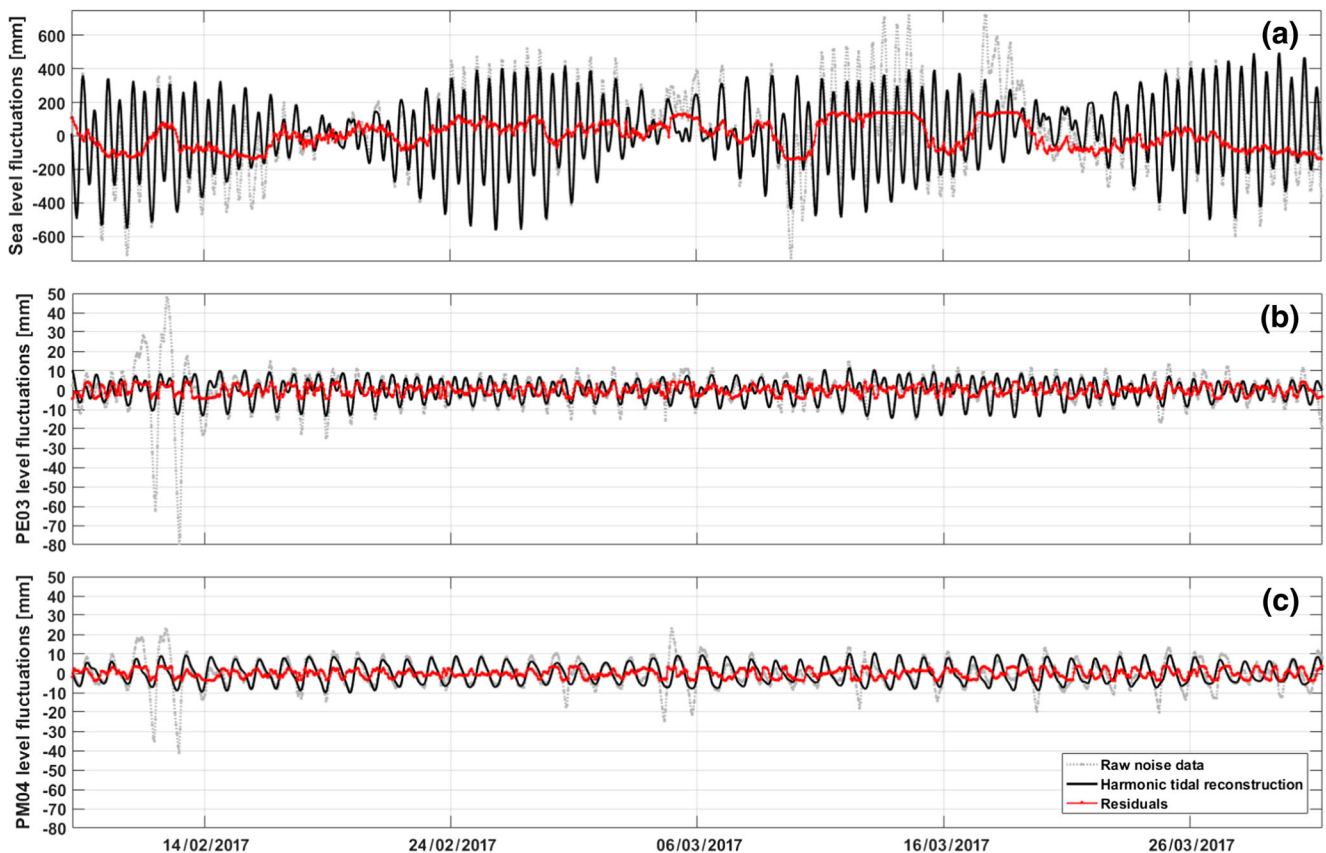


Fig. 11 Signal reconstruction by harmonic components of **a** South Bay seawater level monitoring, and the **b** PE03 and **c** PM04 high frequency signal. In each graph a comparison of raw high frequencies records (gray

dotted lines), tidally reconstructed signal (black solid line) and non-tidally explained residuals (red line) is shown

and PM04 hydraulic head in comparison to the other aperiodic forcings, like rainfall infiltration (Fig. 3). In fact, the absolute value of the reconstructed signals remains confined within 12.2 mm (sygizial tides) and -9 mm (quadrature tides). Nevertheless, analysis of harmonic components on the high frequency residuals allows a quantitative assessment of tidal influence on PE03 and PM04 hydraulic head.

Since the tide estimation uses a 51-day time series, 35 harmonic components are identified. However, when applying significance limits ($\text{SNR} = 6$ and $\text{PE} > 0.5\%$), only eight of those components are shown to be relevant in the South Bay signal and only two in the groundwater level records. Astronomical tide assessment on the South Bay shows that 73.6% of the sea level records are explained by high-frequency periodic contribution, while the other 26.4% is due to other meteorological forcings. In the same way, astronomical tide components explain 33.2 and 49.9% of residual signals after LP33 application, on PE03 and PM04, respectively (Fig. 11). It should be noted that PM04 is 180 m away from the river channel, while PE03 is 300 m away (Fig. 4).

This fact indicates a higher percentage of tidal influence on the signal of the closest piezometer to the river and suggests

that only a small part of the tidal perturbation in the South Bay influences water head in the inland piezometers. Most of higher frequency components seem to be smoothed out by pressure propagation in porous media, in accordance with the main theory of incompressible flow: the higher the component frequency, the greater the attenuation in a dissipative media.

In addition, comparative analysis on K1, that is the only relevant component greater than sensors accuracy ($\text{Ampl} \geq 3.5$ mm) in both PE03 and PM04, indicates that perturbations decrease moving inwards (Tables 5 and 6). PE03 showed an attenuation rate higher than PM04, which conserves more amplitude. At the same time, the PE03 signal had more phase delay than PM04. This observation confirms the findings of Mao et al. (2006) and is due to the tidal perturbation pathway, which moves from the estuary along the course of the river toward the center of the domain. Nevertheless, other nonrelevant components (S2 and O1) exhibit an opposite behavior, which may be due to an additional interaction of the PM04 signal with the water level in the artificial trench close by, where no tidal effects are observed.

Table 5 Comparative tidal analysis (amplitudes with 95% confidence interval). Values in *italic* are the relevant components (namely SNR ≥ 6 , PE $\geq 0.5\%$, and Ampl. ≥ 3.5 mm)

Tidal component Name	Freq. (cl/h) ^c	South Bay (OUT)			PM04 (IN1)				PE03 (IN2)			
		Ampl. (mm)	Ampl. error	Perc. Ener. ^a	Ampl. (mm)	Ampl. error (mm)	Perc. Ener. ^a	Atten. PM04	Ampl. (mm)	Ampl. error (mm)	Perc. Ener. ^a	Atten. ^b PE03
Q1	0.037	<i>26.6</i>	<i>11.3</i>	<i>0.8%</i>	0.9	0.3	1.2%	96.6%	0.9	0.3	1.2%	96.5%
O1	0.039	<i>117.0</i>	<i>9.7</i>	<i>15.6%</i>	0.3	0.3	0.1%	99.8%	1.3	0.3	2.4%	98.9%
K1	0.042	<i>42.4</i>	<i>10.4</i>	<i>2.1%</i>	7.8	<i>0.3</i>	<i>85.6%</i>	<i>81.7%</i>	4.8	<i>0.3</i>	<i>32.4%</i>	<i>88.6%</i>
N2	0.079	<i>39.2</i>	<i>8.2</i>	<i>1.8%</i>	0.1	0.2	0.0%	99.6%	0.3	0.3	0.2%	99.1%
M2	0.081	<i>193.0</i>	<i>8.2</i>	<i>42.8%</i>	0.2	0.2	0.1%	99.9%	0.3	0.3	0.1%	99.8%
S2	0.083	<i>166.0</i>	<i>8.6</i>	<i>31.5%</i>	1.7	0.3	3.9%	99.0%	5.8	<i>0.3</i>	<i>47.3%</i>	<i>96.5%</i>
M3	0.121	<i>24.4</i>	<i>7.1</i>	<i>0.7%</i>	0.2	0.2	0.0%	99.3%	0.1	0.2	0.0%	99.7%
M4	0.161	<i>23.0</i>	<i>8.1</i>	<i>0.6%</i>	0.1	0.2	0.1%	99.4%	0.1	0.2	0.0%	99.6%

^a *Perc. Ener.* is the percent of energy (PE) that contributes to the signal reconstruction as the ratio between component energy, gauge of potential energy of sea level, and total energy of the reconstructed signal

^b *Atten.* is the attenuation of the component in comparison of the South Bay signal. It is calculated by 100 minus the ratio of component amplitude in the piezometer and in the sea-level gauge

^c *cl/h* means cycles per hour. It is a frequency unit that implies a 1/3600 cl/h for a frequency of 1 hertz

Conclusions

The paper describes the use of a time-series approach for WTF, with discrete and irregularly spaced water-level datasets. The application of WTF allowed for the estimation of the groundwater recharge from sparse head records in an aquifer with a shallow water table and sharp fluctuations. The methodology represents an improvement on WTF, increasing its application possibilities. The introduction of a time-variable drainage term and the definition of the differenced water levels based on monitored precipitation allowed for the moderation of the the recharge underestimation with increasing time steps. Hence, the results in the 51-day time

window show good agreement with the results of the Crosbie et al. (2005) method. For the water-level dataset between 2007 and 2017, the estimated amount of recharge is on average 43% of precipitation, showing a higher effectiveness of recharge in the “dry” months with less accumulated rainfall. Subsequently, estimated recharge values are integrated into a 2D finite element model that agrees with observed water level records. Solely low water levels are overestimated in the simulation, probably due to the constant-head BC in the river, suggesting the possibility to introduce a variable-in-time condition to better reproduce dry periods with deeper water table.

The application of WTF is limited to changes in groundwater levels over time due to rainfall infiltration only. This

Table 6 Comparative tidal analysis (phases with 95% confidence interval). Values in *italic* are the relevant components

Tidal component Name	Freq. (cl/h)	South Bay (OUT)			PM04 (IN1)				PE03 (IN2)			
		Pha (360°)	Pha error	SNR (RM) ^a	Pha (360°)	Pha error	SNR (RM) ^a	Δ Pha ^b PM04 (h)	Pha (360°)	Pha error	SNR (RM) ^a	Δ Pha ^b PE03 (h)
Q1	0.037	<i>56</i>	<i>21</i>	<i>22</i>	159	22	34	-7.7	273	22	29	-16.2
O1	0.039	<i>73</i>	<i>5</i>	<i>560</i>	191	81	3	-8.5	347	15	73	-19.6
K1	0.042	<i>150</i>	<i>13</i>	<i>64</i>	<i>166</i>	<i>2</i>	<i>2300</i>	<i>-1.1</i>	<i>221</i>	<i>4</i>	<i>780</i>	<i>-4.7</i>
N2	0.079	<i>145</i>	<i>13</i>	<i>89</i>	359	417	2	-7.5	96	44	6	1.7
M2	0.081	<i>79</i>	<i>3</i>	<i>2100</i>	172	58	5	-3.2	145	58	5	-2.3
S2	0.083	<i>83</i>	<i>3</i>	<i>1400</i>	122	10	150	-1.3	<i>99</i>	<i>9</i>	<i>1700</i>	<i>-0.5</i>
M3	0.121	<i>174</i>	<i>18</i>	<i>46</i>	99	82	1	1.7	223	158	1	-1.1
M4	0.161	<i>99</i>	<i>21</i>	<i>31</i>	276	95	3	-3.1	113	147	1	-0.2

^a *SNR (RM)*: signal-to-noise ratio with modified Rayleigh criterion

^b Δ *Pha*: phase delay between the offshore component in the South Bay and the same component in the piezometer

condition is confirmed to be reasonable at the Ressacada Farm site, by analyzing tidal influence on groundwater levels and absolute values of the residual high-frequency signal in the piezometers, which was usually less than 2 cm of amplitude. Since WTF was shown to be very sensitive to the specific yield, its value is assessed in the paper with a statistically based framework that integrates punctual field measures. The main requirement of the proposed procedure is to allocate all the accumulated precipitation of each interval to the last day of the interval, as if total rainfall infiltrates and recharges the aquifer at the same time. As the sampling intervals increase, the underestimation of recharge using the cumulative approach increases. This limitation is mitigated by introducing a variable D term to account for the water volume that leaves the aquifer in the same time interval. Finally, another important issue is related to the representativeness of the catchment as a whole. The uniform geological setting made the extrapolation of the relevant processes outside of the head monitoring area possible. Nonetheless, it is warranted to incorporate data from outside of the farm site, most of all in the center of the domain, in order to establish representative values for the watershed.

Acknowledgements The authors want to acknowledge FEESC and Petróleo Brasileiro (Petrobras) for the material support that made this study possible and DHI Group for providing a *MIKE Powered by DHI* license file to use FEFLOW. We thank also the Institute of Airspace Control (ICEA) and National Institute of Meteorology (INMET) for providing valuable precipitation data, all the technicians of Agrarian Sciences Center (CCA) for their support in the field data collection, Dr. Luis H. P. Garbossa for help obtaining sea-level records from the EPAGRI/CIRAM gauge station in the South Bay, and the PhD student Martina Pacifici (USP, PPGEC) for help in figure design. Finally, the manuscript benefited from suggestions from two anonymous reviews and comments/discussions with Sue Duncan (technical editorial advisor of *Hydrogeology Journal*) for which we are most grateful.

Funding Information Additionally, the authors acknowledge FEESC and Petróleo Brasileiro (Petrobras) for the financial support that also made this study possible.

References

- Acharya S, Jawitz JW, Mylavarapu RS (2012) Analytical expressions for drainable and fillable porosity of phreatic aquifers under vertical fluxes from evapotranspiration and recharge. *Water Resour Res* 48:1–15. <https://doi.org/10.1029/2012WR012043>
- Anderson MP, Woessner WW, Hunt RJ (2015) *Applied groundwater modelling*, 2nd edn. Elsevier, Amsterdam, 564 pp
- Armstrong D, Narayan K (1998) *Using groundwater responses to infer recharge*. CSIRO, Canberra, Australia
- Bohke J-K (2002) Groundwater recharge and agricultural contamination. *Hydrogeol J* 10:153–179. <https://doi.org/10.1007/s10040-001-0183-3>
- Cao G, Scanlon BR, Han D, Zheng C (2016) Impacts of thickening unsaturated zone on groundwater recharge in the North China plain. *J Hydrol* 537:260–270. <https://doi.org/10.1016/j.jhydrol.2016.03.049>
- Childs EC (1960) The nonsteady state of the water table in drained land. *J Geophys Res* 65:1–3
- Codiga DL (2011) Unified tidal analysis and prediction using the UTide MATLAB functions. Technical report 2011-01, Graduate School of Oceanography, University of Rhode Island, Narragansett, RI, 59 pp. <ftp://www.po.gso.uri.edu/pub/downloads/codiga/pubs/2011Codiga-UTide-report.Pdf>. Accessed 5 March 2017
- Colombani N, Di Giuseppe D, Faccini B et al (2016) Inferring the interconnections between surface water bodies, tile-drains and an unconfined aquifer–aquitard system: a case study. *J Hydrol* 537:86–95. <https://doi.org/10.1016/j.jhydrol.2016.03.046>
- Corseuil HX, Monier AL, Fernandes M et al (2011a) BTEX plume dynamics following an ethanol blend release: geochemical footprint and thermodynamic constraints on natural attenuation. *Environ Sci Technol* 45:3422–3429. <https://doi.org/10.1021/es104055q>
- Corseuil HX, Monier AL, Fernandes M et al (2011b) BTEX plume dynamics following an ethanol blend release: geochemical footprint and thermodynamic constraints on natural attenuation—supporting information. *Environ Sci Technol* 23. <https://doi.org/10.1117/1.1111.2794018.2>
- Corseuil HX, Gomez DE, Schambeck CM et al (2015) Nitrate addition to groundwater impacted by ethanol-blended fuel accelerates ethanol removal and mitigates the associated metabolic flux dilution and inhibition of BTEX biodegradation. *J Contam Hydrol* 174C:1–9. <https://doi.org/10.1016/j.jconhyd.2014.12.004>
- Crosbie RS, Binning P, Kalma JD (2005) A time series approach to inferring groundwater recharge using the water table fluctuation method. *Water Resour Res* 41:1–9. <https://doi.org/10.1029/2004WR003077>
- Cuthbert MO (2010) An improved time series approach for estimating groundwater recharge from groundwater level fluctuations. *Water Resour Res* 46, W09515. <https://doi.org/10.1029/2009WR008572>
- de Vries JJ, Simmers I (2002) Groundwater recharge: an overview of process and challenges. *Hydrogeol J* 10:5–17. <https://doi.org/10.1007/s10040-001-0171-7>
- Delin GN, Healy RW, Lorenz DL, Nimmo JR (2007) Comparison of local- to regional-scale estimates of ground-water recharge in Minnesota, USA. *J Hydrol* 334:231–249. <https://doi.org/10.1016/j.jhydrol.2006.10.010>
- Diersch H-JG (2014) *FEFLOW: finite element modeling of flow, mass and heat transport in porous and fractured media*. Springer, Heidelberg, Germany, 996 pp
- Duke HR (1972) Capillary properties of soils: influence upon specific yield. *Trans ASAE* 15:688–691
- Eching SO, Hopmans JW (1993) Optimization of hydraulic functions from transient outflow and soil water pressure data. *Soil Sci Soc Am J* 57:1167–1175
- Emery WJ, Thomson RE (2001) *Data analysis methods in physical oceanography*, 2nd edn. Elsevier, Amsterdam
- Garbossa LHP, Vanz A, Fernandes L, et al. (2014) Modelling and validation of the Santa Catarina Island bays hydrodynamics based on astronomic tides and measured tides. 11th Int. Conf. Hydroinformatics 8. <https://doi.org/10.13140/2.1.5123.6163>
- Grimm AM, Ferraz SET, Gomes J (1998) Precipitation anomalies in southern Brazil associated with El Niño and La Niña events. *J Clim* 11:2863–2880. [https://doi.org/10.1175/1520-0442\(1998\)011<2863:PAISBA>2.0.CO;2](https://doi.org/10.1175/1520-0442(1998)011<2863:PAISBA>2.0.CO;2)
- Healy RW (2010) *Estimating groundwater recharge*. Cambridge University Press, Cambridge, 245 pp. Available at <https://www.cambridge.org/core/terms>. <https://doi.org/10.1017/CBO9780511780745.001>. Accessed 12 September 2017
- Healy RW, Cook PG (2002) Using groundwater levels to estimate recharge. *Hydrogeol J* 10:91–109. <https://doi.org/10.1007/s10040-001-0178-0>
- Heilweil VM, Benoit J, Healy RW (2015) Variably saturated groundwater modelling for optimizing managed aquifer recharge using trench infiltration. *Hydrol Process* 29:3010–3019. <https://doi.org/10.1002/hyp.10413>

- Hilberts AGJ, Troch PA, Paniconi C, Boll J (2007) Low-dimensional modeling of hillslope subsurface flow: relationship between rainfall, recharge, and unsaturated storage dynamics. *Water Resour Res* 43: 1–14. <https://doi.org/10.1029/2006WR004964>
- Huang FK, Chuang MH, Wang GS, Der Yeh H (2015) Tide-induced groundwater level fluctuation in a U-shaped coastal aquifer. *J Hydrol* 530:291–305. <https://doi.org/10.1016/j.jhydrol.2015.09.032>
- Hunt RJ, Prudic DE, Walker JF, Anderson MP (2008) Importance of unsaturated zone flow for simulating recharge in a humid climate. *Ground Water* 46:551–560. <https://doi.org/10.1111/j.1745-6584.2007.00427.x>
- Kim K, Anderson MP, Bowser CJ (2000) Enhanced dispersion in groundwater caused by temporal changes in recharge rate and lake levels. *Adv Water Resour* 23:625–635. [https://doi.org/10.1016/S0309-1708\(99\)00050-0](https://doi.org/10.1016/S0309-1708(99)00050-0)
- Kobiyama M, Bortolotto NL, Tanaka SI (2011) Relatório Hidrológico da Fazenda experimental da Ressacada [Hydrological report of the Ressacada Experimental Farm]. Centro de Ciências Agrárias, UFSC, Florianópolis, Brazil. Available at <http://fazenda.ufsc.br/descricao-fisica/hidrologia/>. Accessed 1 October 2017
- De Lage IC (2005) Avaliação de metodologias para determinação da permeabilidade em meios porosos: Fazenda Ressacada [Evaluation of methodologies for determination of permeability in porous media: Ressacada Farm]. MSc Thesis, UFRJ, Rio de Janeiro, Brazil
- Lorenz DL, Delin GN (2007) A regression model to estimate regional ground water recharge. *Ground Water* 45:196–208. <https://doi.org/10.1111/j.1745-6584.2006.00273.x>
- Mao X, Enot P, Barry DA et al (2006) Tidal influence on behaviour of a coastal aquifer adjacent to a low-relief estuary. *J Hydrol* 327:110–127. <https://doi.org/10.1016/j.jhydrol.2005.11.030>
- Masetti M, Pedretti D, Sorichetta A et al (2016) Impact of a storm-water infiltration basin on the recharge dynamics in a highly permeable aquifer. *Water Resour Manag* 30:149–165. <https://doi.org/10.1007/s11269-015-1151-3>
- Nachabe MH (2002) Analytical expressions for transient specific yield and shallow water table drainage. *Water Resour Res* 38(10):1193. <https://doi.org/10.1029/2001WR001071>
- Neto DC, Chang HK, van Genuchten MT (2015) A mathematical view of water table fluctuations in a shallow aquifer in Brazil. *Groundwater* 54:82–91. <https://doi.org/10.1111/gwat.12329>
- Park E, Parker JC (2008) A simple model for water table fluctuations in response to precipitation. *J Hydrol* 356:344–349. <https://doi.org/10.1016/j.jhydrol.2008.04.022>
- Peel MC, Finlayson BL, McMahon TA (2006) Updated world map of the Köppen-Geiger climate classification. *Hydrol Earth Syst Sci* 15: 259–263. <https://doi.org/10.1127/0941-2948/2006/0130>
- Pugh DT (1987) Tides, surges and mean sea level. Wiley, Swindon, UK
- Rama F, Franco D, Corseuil HX (2017) Spatial and temporal analysis of natural drainage in the Ressacada aquifer (Florianópolis, Brazil). *IJESD* 8(9):653–660. <https://doi.org/10.18178/ijesd.2017.8.9.1033>
- Saghravani SR, Yusoff I, Wan Md Tahir WZ, Othman Z (2015) Comparison of water table fluctuation and chloride mass balance methods for recharge estimation in a tropical rainforest climate: a case study from Kelantan River catchment, Malaysia. *Environ Earth Sci* 73:4419–4428. <https://doi.org/10.1007/s12665-014-3727-2>
- Sanford W (2002) Recharge and groundwater models: an overview. *Hydrogeol J* 10:110–120. <https://doi.org/10.1007/s10040-001-0173-5>
- Scanlon BR, Healy RW, Cook PG (2002) Choosing appropriate techniques for quantifying groundwater recharge. *Hydrogeol J* 10:18–39. <https://doi.org/10.1007/s10040-001-0176-2>
- Shi X, Vaze J, Crosbie R (2015) The controlling factors in the daily and monthly groundwater recharge estimation using the water table fluctuation method [online]. In: 36th Hydrology and Water Resources Symposium: The Art and Science of Water. ACT, Barton, Australia. <http://search.informit.com.au/documentSummary?dn=824177714642772;res=IELENG>. Accessed 1 October 2017
- Tromp-van Meerveld HJ, McDonnell JJ (2006) Threshold relations in subsurface stormflow: 2. the fill and spill hypothesis. *Water Resour Res* 42:W02411. <https://doi.org/10.1029/2004WR003800>
- Walker GR, Gilfedder M, Dawes WR, Rassam DW (2015) Predicting aquifer response time for application in catchment modeling. *Groundwater* 53(3):475–484. <https://doi.org/10.1111/gwat.12219>
- Xiao H, Wang D, Hagen SC, et al (2016) Assessing the impacts of sea-level rise and precipitation change on the surficial aquifer in the low-lying coastal alluvial plains and barrier islands, east-central Florida (USA). *Hydrogeol J* 1791–1806. <https://doi.org/10.1007/s10040-016-1437-4>